

# Non-Contrast-Enhanced Hand MRA Using Multi-directional Flow-Sensitive Dephasing

Z. Fan<sup>1,2</sup>, P. Hodnett<sup>1</sup>, J. Sheehan<sup>1</sup>, X. Bi<sup>3</sup>, S. Zuehlsdorff<sup>3</sup>, J. Carr<sup>1</sup>, and D. Li<sup>1,2</sup>

<sup>1</sup>Radiology, Northwestern University, Chicago, IL, United States, <sup>2</sup>Biomedical Engineering, Northwestern University, Evanston, IL, United States, <sup>3</sup>Cardiac MR R&D, Siemens Healthcare, Chicago, IL, United States

**Introduction:** Noncontrast hand MRA using ECG-triggered 3D bSSFP with flow-sensitive dephasing (FSD) preparation has recently been demonstrated in patients with Raynauds disease [1]. As with previous studies using FSD preparation [2, 3], the flow-sensitizing gradient pulses were applied in both readout (RO) and phase-encoding (PE) directions simultaneously in order to impart flow-sensitization to in-plane flows when using a coronal acquisition. However, this gradient pulse configuration renders the flow-sensitivity of the FSD module to be a single direction, as derived from the vector sum of the FSD gradients (**Fig. 1**). If blood flow is perpendicular to the FSD direction, there will be no blood signal suppression. In this work, we proposed a new FSD preparative module in an attempt to reliably suppress complex blood flows. Its effectiveness was verified on a flow phantom and healthy volunteers. It was also compared with contrast-enhanced MRA (CE-MRA) in hand imaging of volunteers.

**Materials and Methods: - Pulse sequence** The new FSD preparative module consists of two FSD sub-modules with the gradient pulses applied along the RO direction only in the first module and along the PE direction only in the second one (**Fig. 2**). The dark-artery measurement was acquired with both sub-modules using the same first-order gradient moment ( $m_1$ ) value determined using an  $m_1$ -scout scan; the bright-artery measurement was acquired with all FSD gradient pulses switched off.

**- Flow phantom study** Gd-doped water (0.25mM,  $T_1 = 670$  ms) was pumped (flow rate = 40 cm/s) through a silicone tube (4.8-mm ID). Two perpendicular segments (after sufficiently long transition) of the tube were put in a water bath and imaged on a 1.5T MR system (Espree, Siemens) with a 6-channel body matrix coil. A conventional one-module FSD sequence (**FSD1**) (with FSD pulses applied in both RO and PE simultaneously) and the two-module FSD sequence (**FSD2**) were used for 3D MRA. Spatial resolution was  $0.94 \times 0.94 \times 0.94$  mm<sup>3</sup>, simulated R-R interval = 1000 ms.

**- Healthy volunteer study** (10 subjects, aged 24-57y, mean age = 35 y). Bilateral hand imaging was performed using an oblique coronal acquisition. Two noncontrast MRA scans (FSD1 and FSD2, the order was randomized) preceded a high-resolution CE-MRA scan (0.15 mmol/kg bodyweight Magnevist injected at 2 ml/s, 2 consecutive 22 s-long post-injection measurements, TWIST for bolus timing) at 1.5T. All MRA scans used two body matrix coils with the hands sandwiched between them, 0.94 mm isotropic spatial resolution, and parallel imaging (factor =2).

**- Image analysis** Subtracted 3D data sets and MIP MRA were blindly reviewed by a radiologist on a workstation (Leonardo, Siemens). Overall image quality (IQ) was assessed on a four-point scale (0: not visualized; 3: excellent); venous contamination was assessed on a 3-point scale (0: absent; 2: present, affecting image interpretation); motion was assessed for palm and digits, separately based on a 4-point scale (0: absent; 3: severe, rendering images nondiagnostic) [4]. On each hand, vessel conspicuity was also assessed (score: 0-3) for 15 segments, including superficial arch, deep arch, common digital (3: index/middle, middle/ring, ring/little), princeps pollicis, radialis indicis, proper digital in the index (2: medial and lateral), middle (2), ring (2), and little finger (2). In addition, whether a digit could be visualized to the terminal third was recorded. Wilcoxon signed ranks test was used.

**Results: FSD1 vs FSD2** Flow phantom images showed that the FSD1 module is only sensitive to the flow coinciding with the vector sum of the FSD gradients, whereas the FSD2 module has no this limitation (**Fig. 3**). Nine subjects had successful FSD1 and FSD2. As expected, certain signal loss on MIP images in some segments were observed with FSD1, which was markedly improved with FSD2 (**Fig. 4, 5**). Vessel conspicuity: in 7 segments of the right hands (RH), FSD2 outperformed FSD1, no significant difference in the other 8 segments; in 9 segments of the left hands (LH), FSD2 outperformed FSD1 with one segment showing significant improvement (little finger medial,  $p < 0.05$ ), no significant difference in the other 6 segments.

**FSD2 vs CE-MRA** Eight out of 10 subjects had both FSD2 and CE-MRA data sets. Segments visualized: 101 vs 98 with 95 in common at RH, 100 vs 104 with 97 in common at LH. Vessel conspicuity: no significant difference at both RH and LH. Terminal third visualized: 32/72 vs 8/72. The comparisons of IQ, venous contamination, and motion are summarized in **Table 1**.

**Conclusions:** The new FSD module can reliably suppress multi-directional blood flows and enable comparable vessel delineation with CE-MRA. Superior depiction of the terminal third of the digital artery with FSD-MRA potentially makes this technique more suitable for patients with Raynauds disease.

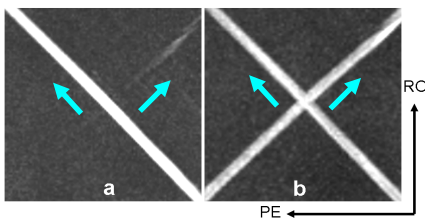


**Fig 3.** Phantom (two perpendicular flows, arrows) subtraction MIP obtained using FSD1(a) and FSD2 (b)

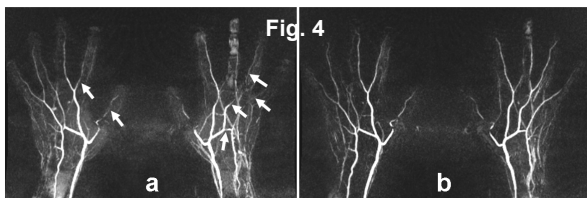


**Fig 4 and 5.** FSD2 (b) depicted more conspicuous segments than FSD1 (a), as marked by arrows on the FSD1 images.

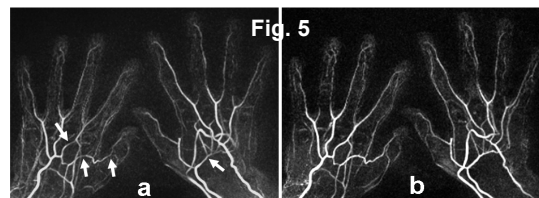


**Fig 4 and 5.** FSD2 (b) depicted more conspicuous segments than FSD1 (a), as marked by arrows on the FSD1 images.

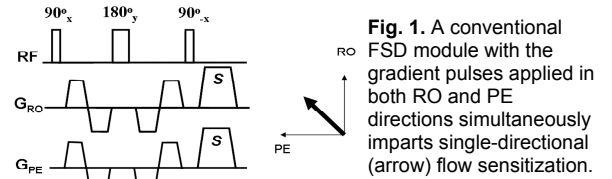


**Fig. 1.** A conventional FSD module with the gradient pulses applied in both RO and PE directions simultaneously imparts single-directional (arrow) flow sensitization.

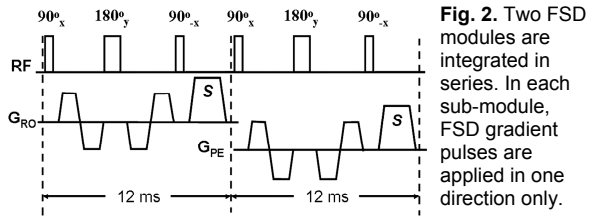


**Fig. 2.** Two FSD modules are integrated in series. In each sub-module, FSD gradient pulses are applied in one direction only.

**Table 1**

	IQ	Venous	Motion (Digits)
FSD1	1.8±0.7	0.7±0.7	1.2±1.1
FSD2	2.4±0.5	0.2±0.4	1.3±1.2
P value	0.03	0.16	0.32
FSD2	2.4±0.5	0.3±0.5	1.4±1.3
CE-MRA	2.1±0.8	1.1±0.8	0
P value	0.41	0.05	0.04

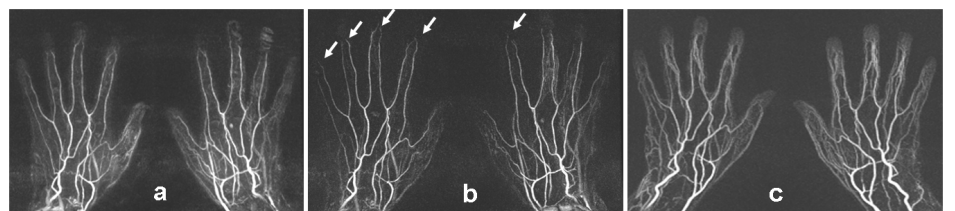


**Fig 6.** MRA with FSD1 (a), FSD2 (b), and CE-MRA (c). More digits exhibited terminal third (arrow) with FSD.

## References:

1. Sheehan J et al. ISMRM 2009 (#423).
2. Sirol M et al. Circulation 2004; 109:2890-96
3. Koktzoglou I et al. JCMR 2007;9:33.
4. Lim RP et al. Radiology 2009: 252:874-81.